Proximity influence of a ferromagnet on the magnetoresistance of Cr film across a nonmagnetic layer

Ciaran McEvoy, Xuesong Jin [a)], I.V. Shvets

SFI Nanoscience Laboratories, Physics Department, Trinity College Dublin, Dublin 2, Ireland

[a)] Corresponding author: Tel: +00 353 1 608 3031

Fax: +00 353 1 671 1759

E-mail: xuesongj@tcd.ie

Abstract

(5 nm) Cr (100)/(x nm) MgO (100)/(30 nm) Fe_3O_4 (100) (1< x < 6 nm), as well as (5 nm) Cr (100)/(5 nm) MgO (100) structures were grown on MgO (100) substrates using molecular beam epitaxy. The proximity influence of the Fe_3O_4 bottom layer on the in-plane transport and magnetotransport properties of the Cr layer was studied. A reversal of the magnetoresistance (MR) sign in the Cr film was observed for MgO layer thickness ≤ 5nm. The thickness of the MgO layer at which the proximity influence of the Fe_3O_4 on the MR of the Cr film is still observed is too large to be accounted for by an exchange interaction. Our results suggest that the magnetic structure in the Cr film adjoining a pinhole in the MgO layer is distorted due to the exchange coupling. Such areas in the Cr film are thought to contribute to the negative MR.

PACS: 75.47.-m, 75.70.-I, 75.70.Cn

Keywords: Magnetoresistance, magnetite, Cr, nonmagnetic insulating layer, direct magnetic coupling

1. Introduction

Spin dependent tunneling between two ferromagnetic (FM) films across an insulator has significant potential for applications in digital storage devices and magnetic sensor technologies [1-4]. Magnetoresistance greater than 20% has been reported in spin tunnel

junctions at room temperature [5-7]. The magnitude of the tunneling MR (TMR) at low temperatures is in close agreement with the predictions of Julliere's model [8]. This model is based on the difference in the density of states of the two spin directions at E_F of the migratory electrons in the two FM electrodes [9]. A large TMR is predicted when a FM electrode with a high spin polarization around the Fermi Level (E_F) is employed [10]. Magnetite (Fe_3O_4), due to its half metallic nature, has attracted much attention as a potential material for magnetic electrode layers in tunneling junctions [11-15]. It was also suggested that spin-dependent tunneling might occur between a ferromagnetic and antiferromagnetic material [16]. In that model a Cr electrode was considered to be an antiferromagnetic layer.

For tunnel junction devices based on a magnetite electrode, MgO has potential as an insulating layer because of the small lattice mismatch (0.3%) between MgO and Fe_3O_4. There have been reports detailing the experimental results for the epitaxial growth of MgO on Fe_3O_4 [17-19]. To fully appreciate and understand the role of MgO as a dielectric in tunnel junctions the magnetic interlayer coupling between the FM electrodes across the MgO layer must be understood. There are several reports on investigation of interlayer coupling across the MgO layer. Slonczeswski proposed a theoretical model according to which spin-polarised conduction electrons of one- or two-band metallic semi-infinite magnetic layers tunnel from one layer to another across a nonmagnetic insulating layer [20]. As a result of this spin-polarised tunneling an effective Heisenberg-like interlayer coupling between the magnetizations of the magnetic layers across a nonmagnetic insulator was predicted. The coupling is either ferromagnetic or antiferromagnetic and its strength decreases rapidly with increasing interlayer thickness. We addressed the issue of coupling *across* an MgO layer in a previous experimental study [21]. That study employed a polycrystalline spinel, $Mn_{0.52}Zn_{0.48}Fe_2O_4$ (MnZn-ferrite), as the FM electrode. The subsequent layers, Cr and MgO, in the structures studied were also polycrystalline. The aim of the present work is to expand the study to an epitaxial film system. Specifically we aim to investigate the influence of the epitaxial half-metallic ferromagnetic layer *on* the MR of the Cr film through the epitaxial MgO spacer layer and to establish how this influence is affected by the thickness of the MgO layer.

The present work was carried out using (5 nm) Cr/(x nm) MgO/(30 nm) Fe_3O_4 (1< x < 6 nm) as well as (5 nm) Cr/(5 nm) MgO structures both grown on MgO (100) single crystal substrates. Magnetite (Fe_3O_4), besides being an interesting half-metallic ferromagnet was chosen as the bottom layer because its resistivity is highly temperature dependent. This makes it possible to investigate the effect of the interlayer coupling on the transport properties of the Cr film when no current flows through the bottom layer at low temperature.

The Cr film was chosen because of its low MR value. Studies have been reported on the magnetic structure of epitaxial Cr films [22-24]. Many of these studies were initiated due to the recent interest in Fe/Cr multilayers and superlattices. It has been reported that epitaxial thin films of Cr for thickness less than 10 nm exhibit commensurate antiferromagnetic characteristics [22]. The expectation was that any influence of the bottom layer (Fe_3O_4) on the top Cr layer through the nonmagnetic spacer layer (MgO) would be readily observable.

2. Experiment

The (5 nm) Cr (100)/(x nm) MgO (100)/(30 nm) Fe_3O_4 (100) and (5 nm) Cr (100)/(5 nm) MgO (100) structures were grown on single crystal MgO substrates by Oxygen-Plasma-Assisted Molecular Beam Epitaxy (MBE) using a DCA Instruments MBE system. The miscut angle of the MgO substrate was less than 0.2º. The base pressure was lower than $5x10^{-10}$ Torr. The MgO substrate was annealed at 600^{o}C for 30 minutes in a plasma oxygen environment prior to deposition. The Fe_3O_4 layer was deposited by means of e-gun evaporation from Fe pellets with a purity of 99.995% in a plasma oxygen environment of $1x10^{-5}$ Torr at a substrate temperature of 250^{o}C. The MgO layer was deposited from MgO pellets of 99.9% purity under similar conditions at a substrate temperature of 400^{o}C. The Cr film was deposited from Cr pellets of purity 99.995% in a vacuum of $5x10^{-8}$ Torr and at a substrate temperature of 250^{o}C. The deposition rates were 0.3, 0.02 and 0.1 Å/s respectively. The low growth rates for MgO and Cr were to promote epitaxial growth. The growth rate was controlled using an INFICON IC-5 process controller and quartz thickness monitors.

The structure of the thin films was characterized by means of High Resolution X-Ray Diffraction (Bede D1 System). The correlation of the interface roughness was studied by means of an X-Ray reflection technique. The transport and magnetotransport properties were investigated using a four-probe method. In all of the experiments outlined below the current was driven in the plane of the film through electrodes attached by means of a conducting epoxy. An external magnetic field up to ~ 1500 kA/m was applied in the plane of the thin film and parallel to the applied current, which is along the (110) direction of the Cr film. The current was supplied by a lock-in-amplifier (Stanford Research System SR 830), which was also used for measurement purposes. An ac current (74 μA) with a frequency of 187 Hz was employed in the present work.

3. Results and Discussion

In-situ reflection high energy electron diffraction (RHEED) patterns were used to monitor the epitaxial growth of the structures. The recorded patterns are presented in Figure 1. Figure 1a shows the RHEED pattern of an MgO (100) substrate. The diffraction pattern shows the vertical surface lattice rods and parabolic Kikuchi lines, indicative of a smooth and ordered surface. Figure 1b shows the half-order lattice rods, located in positions halfway between the locations of the MgO (100) lattice rods. This is indicative of the formation of epitaxial Fe_3O_4 and reflects the double periodicity of the unit cell of Fe_3O_4 compared to MgO. Figure 1c shows the reformation of the MgO (100) pattern as seen in Figure 1a during the growth of the MgO spacer layer. Finally, Figure 1d shows the vertical lattice rods associated with the epitaxial growth of Cr on the MgO spacer layer. The RHEED images demonstrate that heteroepitaxial Cr (100)/MgO (100)/ Fe_3O_4 (100)/MgO (100) structures were obtained.

Figure 2 shows the X-Ray rocking curve for the Fe_3O_4/MgO (100) structure for the symmetric (004) and asymmetric (226) peaks. From the separation of the diffraction peaks it was calculated that the in-plane magnetite lattice parameter, $a_{||}$, was 0.8426 nm and the out-of-plane magnetite lattice parameter, $a_{\perp}$, was 0.8360 nm. The in-plane magnetite lattice parameter, $a_{||}$, was exactly twice that of the MgO lattice parameter (0.4213 nm). This

indicates that the magnetite film grown on the MgO (100) substrate exhibits an out-of-plane compressive strain and a corresponding in-plane tensile strain and that the film was in a fully strained state. It also demonstrates that the magnetite film grew epitaxially on the MgO (100) substrate proving further that heteroepitaxial structures were obtained.

Figure 3 shows the resistivity and magnetoresistance, at a 1500 kA/m field, of the (30 nm) Fe_3O_4 structure on a single crystal MgO (100) substrate as a function of temperature. In this work the magnetoresistance is defined as [R(H)-R(0)]/R(0). The resistance of the magnetite increases greatly with decreasing temperature, as expected. The Verwey transition can be easily observed at ~115K. This value is lower than the Verwey transition temperature for bulk magnetite (~120 K) but this is as expected as there is a trend towards a lower Verwey transition temperature for decreasing film thickness [25, 26]. As the Verwey transition is sensitive to the stoichiometry, its presence in the film demonstrates that the magnetite film is close to the ideal magnetite stoichiometry. Figure 3 also shows that the magnetite film displays a negative MR value. The MR of the magnetite film increases with decreasing temperature. M. Ziese and H. J. Blythe [27] have reported a detailed investigation of the magnetoresistance of single crystal and thin film magnetite.

In this study we focus on the influence on the magnetoresistance of the Cr film caused by the ferromagnetic layer across a nonmagnetic insulating MgO layer. We realized that the MR of the Cr layer might be affected by the possible formation of an alloy caused by interdiffusion at the Cr-MgO interface. To exclude this possibility comparable studies were performed on two systems: Cr/MgO/MgO (100) and Cr/MgO/Fe_3O_4/MgO (100). The two systems were grown under identical conditions at the same (100) MgO substrate temperature and deposition rate. The representative results for the transport and magnetotransport properties of the Cr film in the structure (5 nm) Cr/MgO/MgO (100) substrate are shown in Figure 4. It was found that the resistivity of the Cr film decreases with decreasing temperature, indicative of metallic behaviour. In contrast to the reported value for bulk Cr crystals, a positive MR for the Cr was observed. Adbul-Razzaq and Amoruso [28] reported that a positive MR has been observed for a Cr film with a thickness of 30 nm, again in agreement with the present work.

Figure 5 shows the dependence of the MR at a 1500 kA/m field on the MgO insulator layer thickness at 30K for the (5 nm) Cr/(1-6 nm) MgO/ (30 nm) Fe_3O_4/MgO (100) substrate structure. This is the central result of the present work. In contrast to the positive MR observed for the (5 nm) Cr/(5 nm) MgO/MgO (100) substrate structure, a negative MR is observed for the (5 nm) Cr/ (x nm) MgO/(30 nm) Fe_3O_4/MgO (100) substrate structure for an MgO layer less than 5 nm thick ($\tau_{MgO} \leq$ 5 nm). A positive MR, coinciding with the one observed for the

(5 nm) Cr/MgO/MgO (100) substrate structure, was only observed for $\tau_{MgO} >$ 5 nm. This implies that the influence of the Fe_3O_4 layer on the MR of the Cr film exists for values of $\tau_{MgO} \leq$ 5 nm and vanishes for values of $\tau_{MgO} >$ 5 nm. The MR of the Cr/MgO/Fe_3O_4/MgO (100) substrate structure was linear for a field up to 1500 kA/m, which was the maximum field available for this work. It seems remarkable that the influence of the Fe_3O_4 ferromagnetic bottom layer on the MR of the Cr layer extends across such a thick MgO layer.

It remains to discuss the possible mechanisms responsible for this surprisingly long-range proximity effect. The three mechanisms for consideration are 1) electrical bridging through the pinholes, 2) magnetostatic coupling (“orange peel” coupling) and 3) direct magnetic coupling through the pinholes.

We disregard electrical bridging through the pinholes as a possible mechanism as it could not account for the observed negative MR for the Cr/MgO/Fe_3O_4/MgO (100) structure. This point is explained by expressing the resistance of the Cr film and the magnetite substrate in the presence of the field H as $R_{Cr \text{ or } Fe_3O_4}(H, T) = R_{Cr \text{ or } Fe_3O_4}[1+MR_{Cr \text{ or } Fe3O4}(H, T)]$, where $R_{Cr \text{ or } Fe_3O_4}$ is the resistance at zero field and $MR_{Cr \text{ or } Fe_3O_4}$ (H, T) is the magnetoresistance co-efficient of the Cr film and magnetite substrate respectively under the external magnetic field (H) at temperature (T). Based on the model of two parallel resistors the MR of the entire film-substrate system is:

$$MR_{f-s}(H) = \frac{MR_{Cr}(H,T)\left[1+MR_{Fe_3O_4}(H,T)\right]+\frac{R_{Cr}}{R_{Fe_3O_4}}MR_{Fe_3O_4}(H,T)\left[1+MR_{Cr}(H,T)\right]}{\left[1+MR_{Fe_3O_4}(H,T)\right]+MR_{Fe_3O_4}(H,T)\left[1+MR_{Cr}(H,T)\right]}.$$

The results from this equation are graphed in Figure 6 as a function of the ratio of the film to substrate resistances. The measured values of the MR of epitaxial magnetite and Cr were used for the calculations, these values are –15% and 0.0025% respectively. This clearly demonstrates that the MR of the film-substrate system is largely dependent on the MR of the Cr film provided the ratio $R_{Cr}/R_{Fe_3O_4}$ is small. Typical resistance values for Cr film and magnetite, at 30 K, are 50 Ω and 500 kΩ respectively. This implies a $R_{Cr}/R_{Fe_3O_4}$ ratio of ~$1x10^{-4}$ which, from Figure 6, should yield a positive MR. This is contrary to our experimental observations of a negative MR and thus we conclude that electrical coupling through the pinholes does not play a significant role in the MR of the entire film-substrate system.

The next possible coupling mechanism for discussion is magnetostatic coupling. Neel magnetostatic coupling, also referred to as “orange peel” coupling, results from the correlated interface roughness of the Cr film and magnetite surface. This mechanism has been comprehensively studied recently. The interlayer coupling between Fe_3O_4 layers separated by an MgO insulating layer with thickness in the range 0 - 45 nm has been investigated [29]. Coupling for an MgO layer thicker than 1.3 nm was attributed to the Neel magnetostatic coupling. The magnetic field due to Neel coupling depends on the surface roughness. The X-Ray reflectivity reciprocal space map of the Cr/MgO/Fe_3O_4/MgO substrate structure shown in Figure 7 clearly confirms that there is a good interlayer correlation for the Cr/MgO/Fe_3O_4/MgO (100) structure. This is evidenced from the elongation of the peaks in the reciprocal space map. Such features are indicative of a good interlayer correlation [30-32]. Therefore the basic assumptions for the “orange peel” model were fulfilled for our structures. The coupling field H could be modeled assuming that the surface has a two dimensional sinusoidal waviness with amplitude h and wavelength ω [33],

$$H = \frac{\pi^2 h}{\sqrt{2}\omega} M_s \exp\left(-\frac{2\pi\sqrt{2}}{\omega}t\right),$$

where M_s is the saturation magnetization of the substrate and t is the thickness of the nonmagnetic spacer layer. For demonstration purposes we use the bulk saturation magnetization value for magnetite (470 emu/cm^3). Values for h and ω were determined from AFM measurements of the Cr/MgO/Fe_3O_4/MgO (100) structure. The values thus determined were h=1.5 nm and ω=412 nm.

Calculated results are tabulated in Table 1 and show that the additional field created in the Cr film due to magnetostatic coupling is negligibly small in comparison with the 1500 kA/m field at which the MR of the Cr/MgO/Fe_3O_4/MgO (100) structure was measured and as such we conclude that the effect of magnetostatic coupling cannot explain the reversal of the MR observed.

Thus we suggest, in agreement with earlier studies [21], that the reversal of the MR is due to direct magnetic coupling through the pinholes. The model predicts that the magnetic structure in Cr in the direct vicinity of a pinhole is distorted though an exchange interaction with the magnetite substrate. This is represented schematically in Figure 8. The distortion is affected and modified in the presence of an external magnetic field as the field rotates the magnetization of the Fe_3O_4 region, coupled through the pinhole to the Cr film. The model suggests that the electrons undergo less scattering in the region of distorted magnetic structure, which explains the negative MR observed. Further, it is suggested that the pinhole does not have to be completely open for the exchange interaction between the Cr film and the substrate to lead to a distorted magnetic structure in the Cr film. This would explain the negative MR up to an MgO thickness up to 5 nm, where pinholes may not necessarily exist. Even when a pinhole is not completely open it is reasonable to expect that the Cr and magnetite regions simply need to be positioned in close enough proximity for the exchange interaction to become effective. This is schematically shown in Figure 8c. It was proposed in [20] that pinholes are present in an MgO layer up to a thickness of ~3 nm when the insulating layer is deposited on an MnZn spinel substrate. Study [29] suggests that pinholes exist for an MgO layer up to 1.3 nm thick. It is clear that the critical thickness above, which pinholes no longer exist, depends on the substrate strain status in the MgO film and also on the growth

conditions for the film. However these values indicate that the exchange interaction between the Cr and magnetite is effective even when a 1 to 2 nm thick MgO spacer layer separates them.

4. Conclusions

The influence of the magnetite bottom layer on the in-plane transport and magnetotransport properties of a Cr layer was investigated using a (5 nm) Cr (100)/(1-7 nm) MgO (100) /(30 nm) Fe_3O_4 (100)/MgO (100) epitaxial structure as well as a (5 nm) Cr (100)/(5 nm) MgO (100) epitaxial structure, both grown on MgO (100) single crystal substrates. A distinct proximity influence of the magnetite layer on the Cr film was observed when the thickness of the MgO insulator layer was less than 5 nm. The influence was so extreme that the sign of the MR was reversed, resulting in a negative MR. The effects of electrical coupling through the pinholes and Neel magnetostatic coupling have been excluded as possible mechanisms for the observed negative MR. The model of direct magnetic coupling through the pinholes for such systems appears to be verified by the observed results.

Acknowledgements

This work was supported by Science Foundation Ireland (SFI) under Contract No. 00/PI.1/C042.

References

[1] J. S. Moodera, Lisa R. Kinder, Terrilyn M. Wong, R. Meservey, Phys. Rev. Lett. 74 (1995) 3273

[2] W. J. Gallagher, S. S. P. Parkin, Yu Lu, X. P. Bian, A. Marley, K. P. Roche, R. A. Altman, S. A. Rishton, C. Jahnes, T. M. Shaw, Gang Xiao, J. Appl. Phys. 81 (1997) 3741

[3] M. Sato, K. Kobayashi, Jpn. J. Appl. Phys. Part 1 36 (1997) 200

[4] J. M. Daughton, J. Appl. Phys. 81 (1997) 3758

[5] S. S. P. Parkin, K. P. Roche, M. G. Samant, P. M. Rice, R. B. Beyers, R. E. Scheuerlein, E. J. O'Sullivan, S. L. Brown, J. Bucchigano, D. W. Abraham, Yu Lu, M. Rooks, P. L. Trouilloud, R. A. Wanner, W. J. Gallagher, J. Appl. Phys. 85 (1999) 5828

[6] Jagadeesh S. Moodera, Janusz Nowak, Rene J. M. van de Veerdonk, Phys. Rev. Lett. 80 (1998) 2941

[7] R. C. Sousa, J. J. Sun, V. Soares, P. P. Freitas, A. Kling, M. F. de Silva, J. C. Soares, J. Appl. Phys. 85 (1999) 5258

[8] M. Julliere, Phys. Lett. A 54 (1975) 225

[9] Mary Beth Stearns, J. Magn. Magn. Mater. 5 (1977) 167

[10] S. F. Alvarado, W. Eib, F. Meier, D. T. Pierce, K. Sattler, H. C. Siegmann, J. P. Remeika, Phys. Rev. Lett. 34 (1975) 319

[11] K. Ghosh, S. B. Ogale, S. P. Pai, M. Robson, Eric Li, I. Jin, Zi-wen Dong, R. L. Greene, R. Ramesh, T. Venkatesan, M. Johnson, Appl. Phys. Lett. 73 (1998) 689

[12] X. W. Li, A. Gupta, Gang Xiao, W. Qian, V. P. Dravid, Appl. Phys. Lett. 73 (1998) 3282

[13] P. Seneor, A. Fert, J-L. Maurice, F. Montaigne, F. Petroff, A. Vaurès, Appl. Phys. Lett. 74 (1999) 4017

[14] P. J. van der Zaag, P. J. H. Bloemen, J. M. Gaines, R. M. Wolf, P. A. A. van der Heijden, R. J. M. van de Veerdonk, W. J. M. de Jonge, J. Magn. Magn. Mater. 211 (2000) 301

[15] Jin Pyo Hong, Sung Bok Lee, Young Woo Jung, Jong Hyun Lee, Kap Soo Yoon, Ki Woong Kim, Chae Ok Kim, Chang Hyo Lee, Myoung Hwa Jung, Appl. Phys. Lett. 83 (2003) 1590

[16] A. A. Minakov, I. V. Shvets, Surface Science 236 3 (1990) L377

[17] P. A. A. van der Heijden, M. G. van Opstal, C. H. W. Swüste, P. H. J. Bloemen, J. M. Gaines, W. J. M. de Jonge, J. Magn. Magn. Mater. 182 (1998) 71

[18] Prasanna Shah, Mitsugu Sohma, Kenji Kawaguchi, Iwao Yamaguchi, J. Magn. Magn. Mater. 247 (2002) 1

[19] F. C. Voogt, T. T. M. Palstra, L. Niesen, O. C. Rogojanu, M. A. James, T. Hibma, Phys. Rev. B 57 (1998) R8107

[20] J. C. Slonczewski, Phys. Rev. B 39 (1989) 6995

[21] Xuesong Jin, I. V. Shvets, J. Appl. Phys. 94 (2003) 5035

[22] E. Kunnen, K. Temst, V. V. Moshchalkov, Y. Bruynseraede, S. Mangin, A. Vantomme, A. Hoser, Physica B 276 (2000) 738

[23] K. Mibu, S. Tanaka, T. Kobayashi, A. Nakanishi, T. Shinjo, J. Magn. Magn. Mater. 198 (1999) 689

[24] Hartmut Zabel, Patrick Bödeker, Andreas Schreyer, J. Phys. D: Appl. Phys. 31 (1998) 656

[25] S. P. Sena, R. A. Lindley, H. J. Blythe, Ch. Sauer, M. Al-Kafarji, G. A. Gehring, J. Magn. Magn. Mater. 176 (1997) 111

[26] G. Q. Gong, A. Gupta, Gang Xiao, W. Qian, V. P. Dravid, Phys. Rev. B 56 (1997) 5096

[27] M. Ziese, H. J. Blythe, J. Phys.: Condens. Matter 12 (2000) 13

[28] W. Abdul-Razzaq, M. Amoruso, Physica B 253 (1998) 47

[29] P. A. A. van der Heijden, P. J. H. Bloemen, J. M. Metselaar, R. M. Wolf, J. M. Gaines, J. T. W. M. van Eemeren, P. J. van der Zaag, W. J. M. de Jonge, Phys. Rev. B 55 (1997) 11569

[30] V. Holý, T. Baumbach, Phys. Rev. B 49 (1994) 10668

[31] V. M. Kaganer, S. A. Stepanov, R. Köhler, Phys. Rev. B 52 (1995) 16369

[32] E. A. Kondrashkina, S. A. Stepanov, R. Opitz, M. Schmidbauer, R. Köhler, R. Hey, M. Wassermeier, D. V. Novikov, Phys. Rev. B 56 (1997) 10469

[33] J. C. S. Kools, W. Kula, Daniele Mauri, Tsann Lin, J. Appl. Phys. 85 (1999) 4466

Figure Captions

Figure 1. RHEED patterns of (a) cleaned MgO (100) substrate, (b) after growth of the 10 nm thick Fe_3O_4 bottom layer, (c) after growth of the 1 nm MgO spacer layer, and (d) after growth of the 5 nm top Cr layer. All patterns were recorded along the <011> azimuth at electron beam energy of 20 kV.

Figure 2. X-Ray Diffraction Rocking curves for the symmetric (004) and asymmetric (226) peaks of the 30 nm thick magnetite film. The higher intensity peaks are the (002) and (113) peaks of the MgO (100) substrate.

Figure 3. Resistivity and magnetoresistance at a 1500 kA/m field of the 30 nm magnetite film as a function of temperature. The line joining the magnetoresistance data points is added as a guide for the eye.

Figure 4. Resistivity and magnetoresistance at a 1500 kA/m field of the 5 nm Cr thin film as a function of temperature. The line joining the magnetoresistance data points is added as a guide for the eye.

Figure 5. Dependence of the magnetoresistance of the (5 nm) Cr/(1-6 nm) MgO/(30 nm) Fe_3O_4/MgO (100) structure at a field strength of 1500 kA/m and a temperature of 30 K.

Figure 6. Calculated magnetoresistance of the Cr film-Magnetite layer system as a function of film to substrate resistance ratio ($R_{Cr}/R_{Fe_3O_4}$). The line joining the magnetoresistance data points is added as a guide for the eye.

Figure 7. X-Ray reflectivity reciprocal space map for the structure: (5 nm) Cr/(1 nm) MgO/(30 nm) Fe_3O_4/MgO (100) substrate.

Figure 8. (a) Schematic diagram of a pinhole. The material in the pinhole forms a domain coupled to the Cr film by exchange interaction. The external field is zero. (b) External magnetic field is applied. This rotates the magnetic moments in the magnetite in the pinhole area and also spins in the Cr layer, which are coupled by exchange with the magnetite. This creates an area with a distorted magnetic structure where the electrons traveling in the Cr film undergo less scattering. (c) The case when a pinhole is not completely open, i.e. there is a thin layer of MgO preventing electric contact between the Cr and magnetite substrate but still placing the two in close proximity.

t (nm)	H (mT)
1	14.7
3	14.1
5	13.5

Table 1. Calculated coupling field based on the “orange peel” model

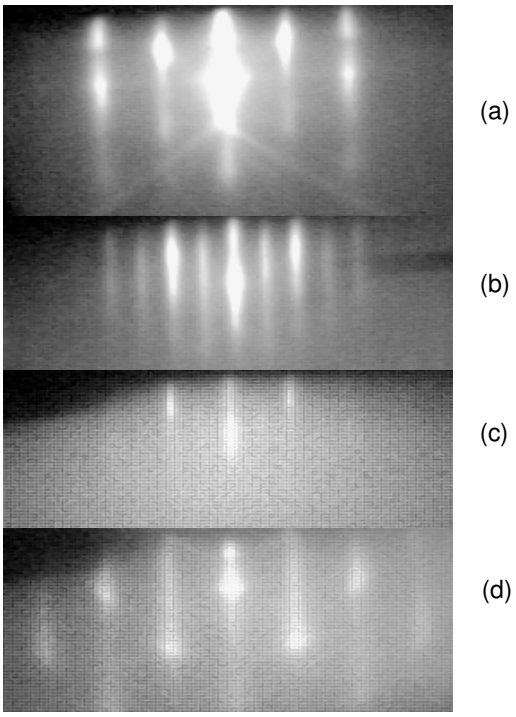

Figure 1 Submitted to J. Magn. Magn. Mater.

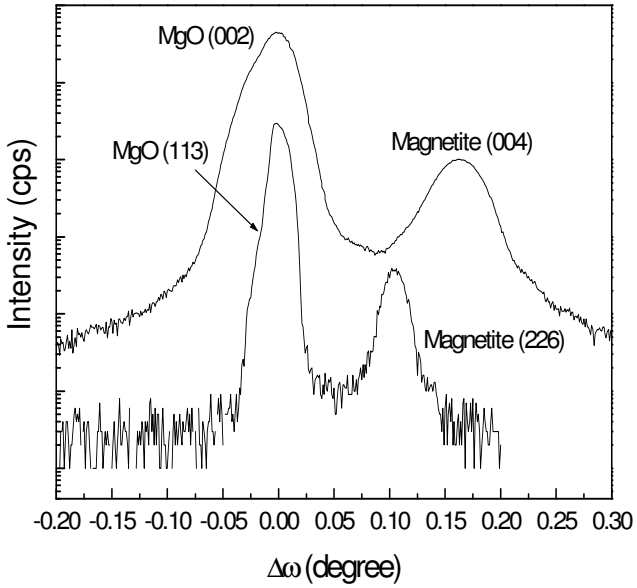

Figure 2. Submitted to J. Magn. Magn. Mater

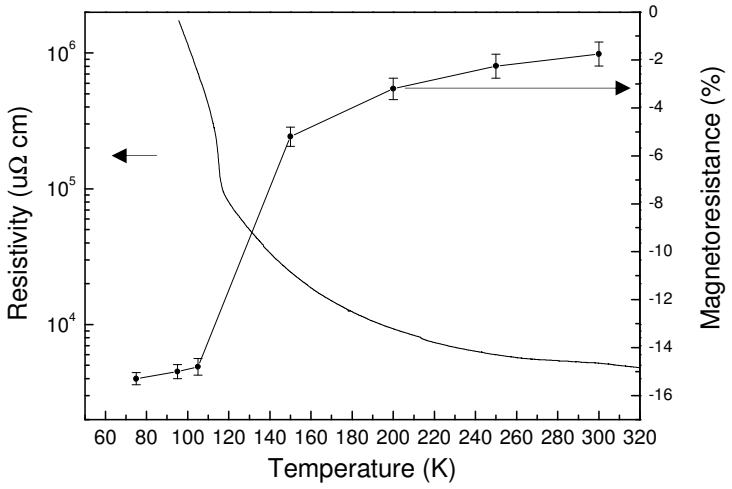

Figure 3. Submitted to J. Magn. Magn. Mater

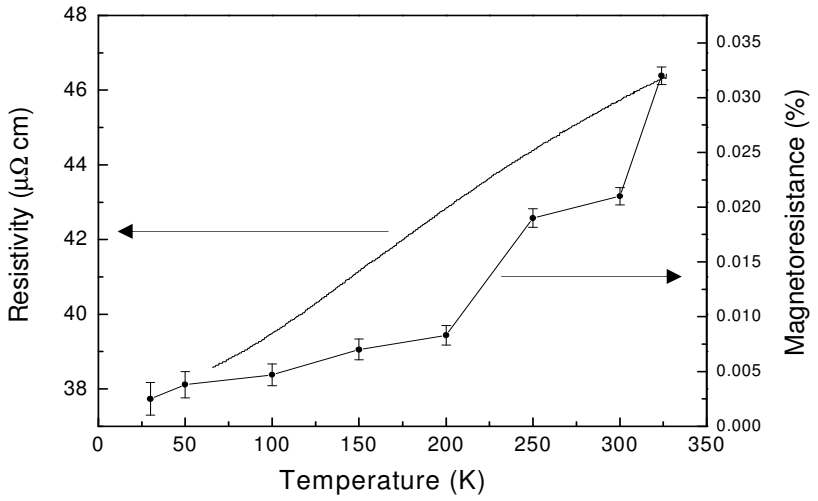

Figure 4. Submitted to J. Magn. Magn. Mater

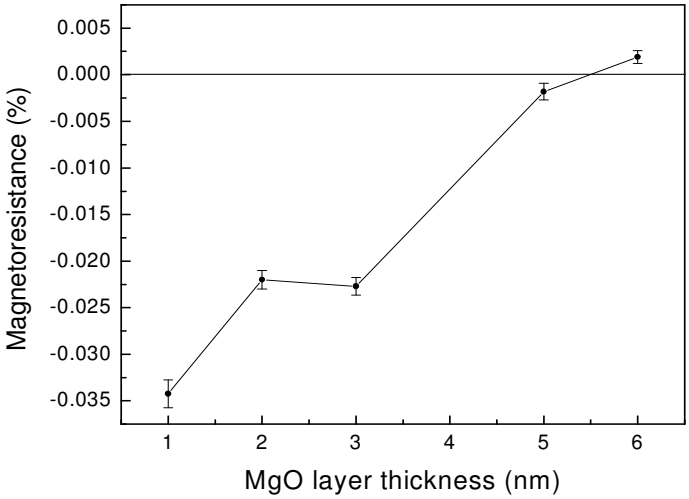

Figure 5. Submitted to J. Magn. Magn. Mater

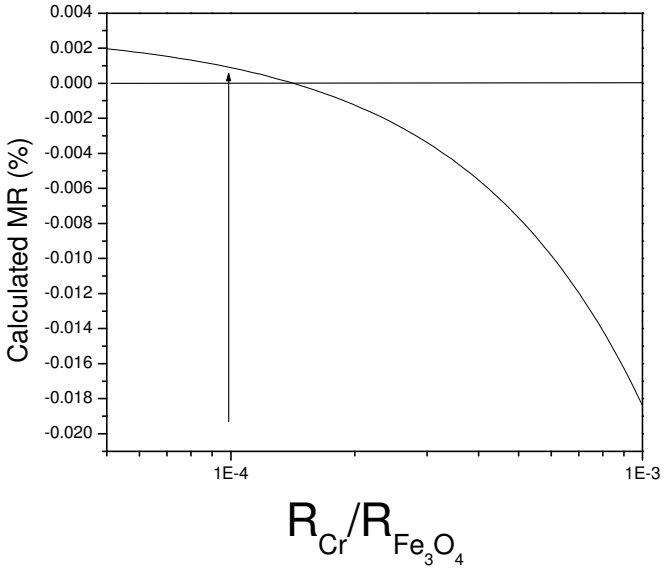

Figure 6. Submitted to J. Magn. Magn. Mater.

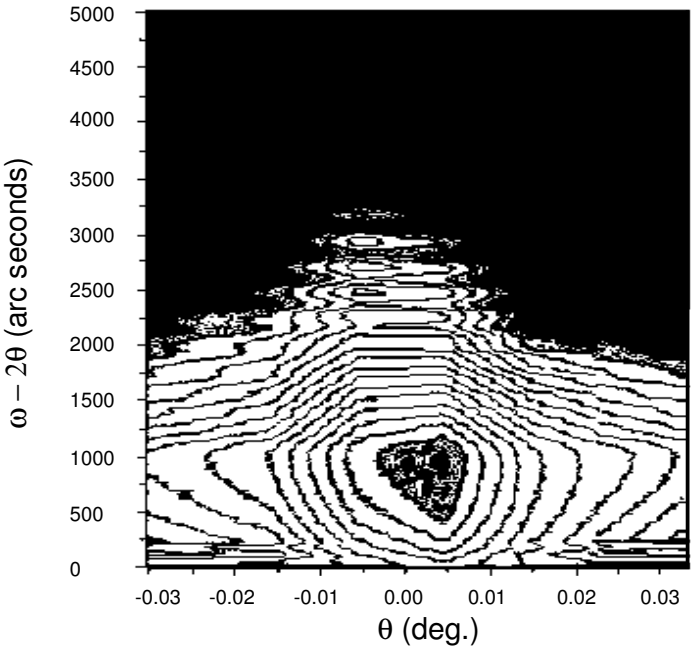

Figure 7. Submitted to J. Magn. Magn. Mater

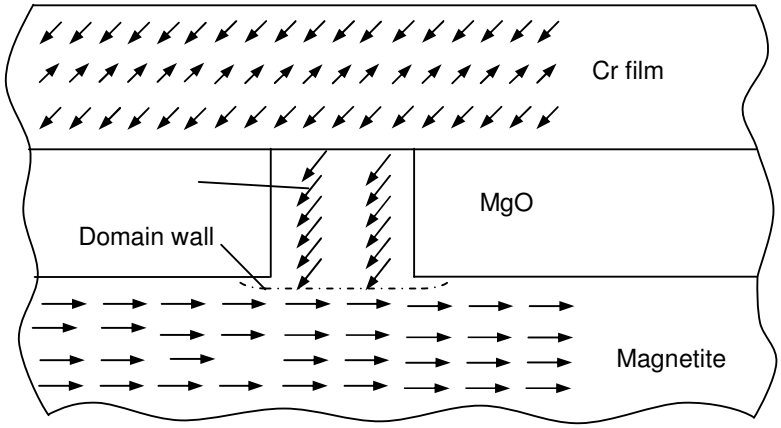

(a)

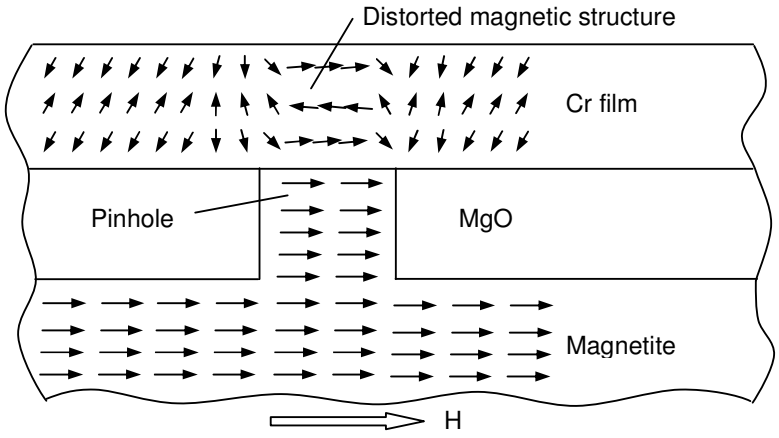

(b)

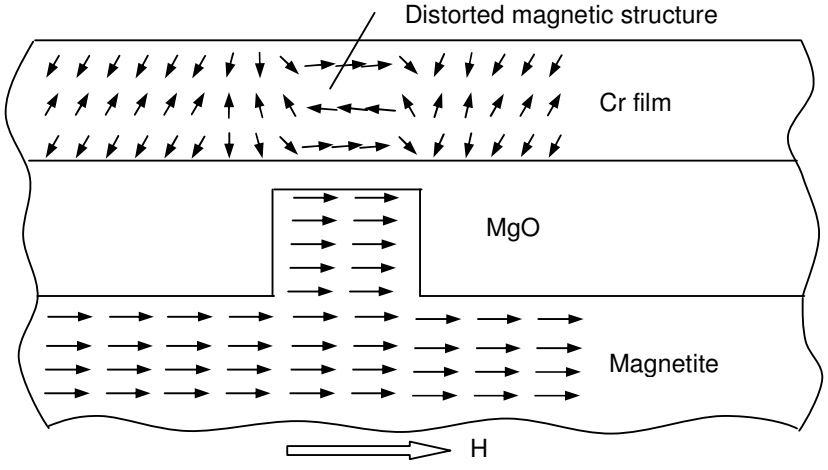

(c)

Figure 8. Submitted to J.Magn. Magn. Mater.